

Many-body dynamics of p -wave Feshbach molecule production: a mean-field approach

L. Austen,¹ L. Cook,¹ M. D. Lee,² and J. Mur-Petit^{3,*}

¹*Department of Physics and Astronomy, UCL, Gower Street, WC1E 6BT London, United Kingdom*

²*School of Mathematics, University of Southampton, Southampton SO17 1BJ, United Kingdom*

³*Instituto de Física Fundamental, IFF-CSIC, Serrano 113 bis, 28006 Madrid, Spain*

We study the mean-field dynamics of p -wave Feshbach molecule production in an ultra-cold gas of Fermi atoms in the same internal state. We derive a separable potential to describe the low-energy scattering properties of such atoms, and use this potential to solve the mean-field dynamics during a magnetic field sweep. Initially, on the negative scattering length side of a Feshbach resonance the gas is described by the BCS theory. We adapt the method by Szymańska et al. [Phys. Rev. Lett. **94**, 170402 (2005)] to p -wave interacting Fermi gases and model the conversion dynamics of the gas into a Bose-Einstein condensate of molecules on the other side of the resonance under the influence of a linearly varying magnetic field. We have analyzed the dependence of the molecule production efficiency on the density of the gas, temperature, initial value of the magnetic field, and magnetic field ramp speed. Our results show that in this approximation molecule production by a linear magnetic field sweep is highly dependent on the initial state.

PACS numbers: 03.75.Ss, 05.30.Fk, 34.50.-s

I. INTRODUCTION

Ultra-cold Fermi gases have attracted considerable interest due to the possibility of studying many-body fermionic physics in well controlled and tunable environments [1]. Some of this interest has been stimulated by the prospect of observing pairing phenomena similar to those observed in superconductors and liquid ^3He . The existence of magnetically tunable Feshbach resonances in ultra-cold gases [2–6] allows the interaction strength between the atoms to be tuned such that the system behaves as a gas of long range Cooper pairs described by the theory of superconductivity presented by Bardeen, Cooper and Schrieffer (BCS) [7] in the limit of weak interatomic interaction, and as a Bose-Einstein condensate (BEC) of diatomic molecules in the limit of weak repulsion [8]. The transition between these limits is often referred to as the BCS-BEC crossover [1].

Identical fermions in the same internal state are forbidden from colliding in the s -wave ($\ell=0$, ℓ being the value of the relative angular momentum quantum number) so that the lowest partial wave scattering amplitude becomes the p -wave ($\ell=1$). Pairing between atoms interacting in the p -wave has been theoretically studied in the context of solid-state superconductivity [9], ^3He [10], particle physics [11] and, more recently, ultra-cold gases [12–20]. p -wave Feshbach resonances have been observed in ultra-cold gases of the fermionic isotopes ^{40}K [21] and ^6Li [22, 23]. In the case of ^{40}K experiments have shown the existence of a splitting of the p -wave resonance which was explained by the magnetic dipole-dipole interaction between the atomic valence electrons [24].

The formation of weakly bound diatomic p -wave molecules has been experimentally observed in both ^{40}K [25] and ^6Li [22, 26]. In the work on ^{40}K , atoms were prepared in the state labelled $|f, m_f\rangle = |9/2, -7/2\rangle$, where f denotes the hyperfine state of an atom in the absence of a magnetic field and m_f denotes the Zeeman state of the atom. Molecules were formed using a resonantly modulated magnetic field [25], as first demonstrated for the formation of molecules in Bose gases [27]. Binding energies of the $^{40}\text{K}_2$ molecules were measured on both the BEC side where the atoms form a bound state and on the BCS side where the atoms form a resonance state localised by the centrifugal barrier. In the latter case lifetimes for decay from the resonance state were also measured. Similar experiments in ^6Li used linear sweeps of the magnetic field to form molecules [26, 28, 29].

Motivated by these experiments we study the dynamics of molecule formation from a gas of fermionic atoms in the same internal state, which occurs during a linear sweep of the magnetic field. Such a system has been studied previously by Szymańska et al. [30], who used a mean-field approach to investigate s -wave pairing for fermions in different spin states. Here we extend this treatment to deal with the more complicated p -wave pairing case. The initial state is taken to be a BCS paired gas on the negative scattering length side of the resonance. We study the dependence of the molecule production efficiency on the speed of the magnetic field sweep, as well as on temperature, density and initial magnetic field position. We also study the evolution of the order parameter and the molecule density after a rapid variation of the magnetic field.

This article is structured as follows: In Sec. II, we introduce the pseudo-potential that we use to model the two body physics in the many body problem. In Sec. III, we present our BCS model for studying the initial state of the gas from which to study the dynamics, while Sec. IV contains the dynamical equations. We study

*Electronic address: jordi.mur@csic.es; Present address: Instituto de Estructura de la Materia, IEM-CSIC, Serrano 123, 28006 Madrid, Spain

linear sweeps of the magnetic field from the BCS side of the resonance into the BEC side where we calculate the molecule production efficiency by taking the overlap of the pair function with the two body bound state. We also analyze the prospects to observe atom-molecule coherent oscillations as a function of the time after a fast sweep through the resonance. Finally, Sec. V is a discussion of our results.

II. TWO-BODY MODEL

In order to study the many-body effects present in the formation of p -wave Feshbach molecules as a linear magnetic field sweep is applied across the resonance, we extend the methods of Szymańska et al. [30] to the case of a p -wave resonance. We must therefore choose a suitable representation for the two-body physics. Due to the low energies involved in ultra-cold collisions, it is not necessary to use the exact form of the interatomic potential, provided that all relevant low energy scattering properties are reproduced. Previous work on fermions has been successful in describing the two-body physics of Feshbach resonances using pseudo-potentials in both the s -wave and p -wave [20]. Both the mean-field thermodynamics and dynamics have been studied using a separable potential to model the two-body interaction close to an s -wave Feshbach resonance [30, 31]. Motivated by this we seek a similar separable form of the p -wave potential that can be used in the many-body calculations.

The presence of a magnetic field defines a quantisation axis. Particles interacting in the p -wave have one quantum of relative angular momentum and there are three possible projections of this vector onto the quantisation axis. The situation can be encapsulated in a three-component separable potential

$$V = |\chi_{1,1}\rangle\xi_{1,1}\langle\chi_{1,1}| + |\chi_{1,0}\rangle\xi_{1,0}\langle\chi_{1,0}| + |\chi_{1,-1}\rangle\xi_{1,-1}\langle\chi_{1,-1}|. \quad (1)$$

Here $|\chi_{\ell,m_\ell}\rangle$ is the form factor of the potential and ξ_{ℓ,m_ℓ} is the amplitude, where m_ℓ denotes the projection of this angular momentum onto the magnetic field, which we choose to be in the z -direction. This pseudo-potential can account for the observed splitting of the resonance feature [24] into distinct resonances depending upon the value of $|m_\ell|$, due to magnetic dipole-dipole interactions between the valence electrons. For each individual term a suitable choice must be made for the form factor to recover the low energy scattering behaviour of the atom pair. A model that reproduces the threshold behaviour should be sufficient for our calculations since this is the energy range in which the experiments have been performed.

We set the parameters of the pseudo-potential to reproduce physical observables. One feature of the two body physics that we can compare with experiment is the measured binding energy of the molecule. Bound states are associated with a pole in the T -matrix [32] given by the

Lippmann-Schwinger equation

$$T(z) = V + VG_0(z)T(z). \quad (2)$$

Here $G_0(z) = (z - H_0)^{-1}$ is the free Green's function and H_0 is the free Hamiltonian. Experimental measurements show that the resonances due to the different $|m_\ell|$ values in ^{40}K are narrow and well separated [24], and so we assume each term of Eq. (1) can be treated individually leading to a T -matrix for each component in the form

$$T_{1m_1}(z) = \frac{|\chi_{1m_1}\rangle\xi_{1m_1}\langle\chi_{1m_1}|}{1 - \xi_{1m_1}\langle\chi_{1m_1}|G_0(z)|\chi_{1m_1}\rangle}. \quad (3)$$

A pole in $T_{1m_1}(z)$ coincides with a vanishing denominator in Eq. (3). The T -matrix is related to the scattering amplitude through $f_{\ell,m_\ell}(p) = -\pi m\hbar\langle p\ell, m_\ell|T_{\ell,m_\ell}\left(\frac{p^2}{2\mu} + i0\right)|p\ell, m_\ell\rangle$, where p is the magnitude of the relative momentum and m is the single particle mass. Given that the long range behaviour of the interatomic interaction is dominated by the van der Waals potential [33], the parameter ξ_{1m_1} can be related to the scattering properties of the system from the low-energy limit of the partial wave scattering amplitude for the s -wave and p -wave [34]

$$\lim_{p \rightarrow 0} f_{\ell,m_\ell}(p) = -a_{\ell,m_\ell} \frac{p^{2\ell}}{\hbar^{2\ell}}. \quad (4)$$

Here a_{ℓ,m_ℓ} is the partial wave scattering ‘‘length’’, which in the case of the p -wave has the dimensions of volume and shall here be referred to as the scattering volume. Furthermore, in the vicinity of a resonance the scattering volume can be parameterised by the magnetic field using the well known resonance formula [35, 36]

$$a_{\ell,m_\ell}(B) = a_{\ell,m_\ell}^{\text{bg}} \left(1 - \frac{\Delta B_{\ell,m_\ell}}{B - B_{\ell,m_\ell}^0}\right). \quad (5)$$

Here $a_{\ell,m_\ell}^{\text{bg}}$ is the partial-wave background scattering ‘‘length’’ for the m_ℓ th component, $\Delta B_{\ell,m_\ell}$ is referred to as the width of the resonance and B_{ℓ,m_ℓ}^0 is the resonance position. With this approach, we extend to p -wave interactions earlier work [30, 31] demonstrating that a single-channel approach with this magnetic-field dependence for the scattering length, Eq. (5), is appropriate to describe the dynamics of cold Fermi gases interacting via s -waves.

In Appendix A we discuss how we obtain a suitable p -wave form factor, and give values for the parameters of our separable potential for the case of ^{40}K atoms. Using this potential, we can solve the equation for the bound state

$$1 - \xi_{1m_1}\langle\chi_{1m_1}|G_0(E_{-1})|\chi_{1m_1}\rangle = 0, \quad (6)$$

where E_{-1} is the energy of the least bound state of the atom pair. We then get the low energy expansion of the bound state energy [16]

$$E_{-1} \approx -\frac{\sqrt{\pi}\sigma_{1m_1}\hbar^2}{ma_1}, \quad (7)$$

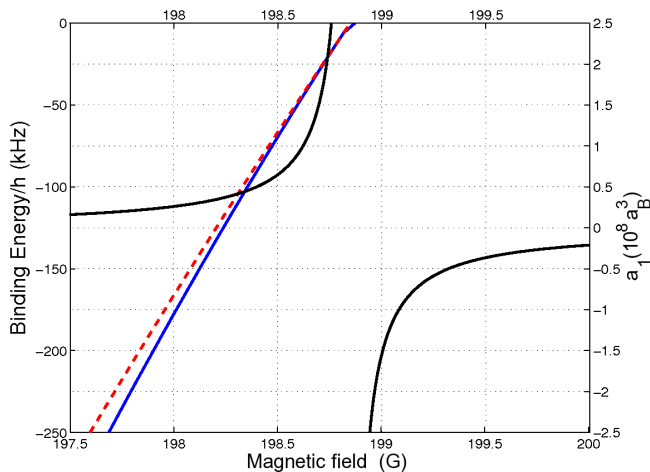


FIG. 1: (Color online) Variation of the p -wave binding energy with the magnetic field for the $m_1 = 0$ resonance in ^{40}K . The solid blue line is the solution to Eq. (A3). The dashed red line is the low energy expansion of Eq. (7). The black solid line shows the variation of the scattering volume (right axis) in the vicinity of the resonance.

where σ_{1m_1} is a parameter associated with the range of the potential, as explained in Appendix A. This expression shows that the bound state energy varies as the inverse of the scattering volume, and to this extent is in agreement with previous two-channel calculations [36–38]. A plot of the bound state energy about the $B_{1,0}^0 = 198.85$ G $m_1 = 0$ resonance in ^{40}K found from Eq. (A3) is given in Fig. 1. Also plotted is the low energy expansion of Eq. (7), which shows a good agreement close to the resonance.

For p -wave resonances, it has been observed that the magnetic dipole-dipole interaction plays an important role, leading for example to the splitting of the $m_1 = 0$ and $m_1 = \pm 1$ resonances [24]. For such an interaction, which decays as $1/r^3$ at long distances, no scattering length can be properly defined [32]. However, a scattering volume model may give the correct scattering cross section behaviour within some finite range of collision energies. Physically this can be regarded as truncating the interaction at the radius where it becomes small compared to the kinetic energy. To illustrate this Fig. 2 shows the scattering cross section given by our pseudo-potential, and compares it to a much more detailed coupled-channels calculation. Here we obtain the coupled-channels results using the Manolopoulos log-derivative propagation technique [39] including a dipole-dipole interaction term in the Hamiltonian [40]; we use the Born-Oppenheimer potentials of ref. [41]. It can be seen that our separable potential reproduces the low energy scattering behaviour to a good degree over several orders of magnitude, particularly close to the resonance, and we therefore proceed in the following sections to use this potential in the many-body problem of molecule formation.

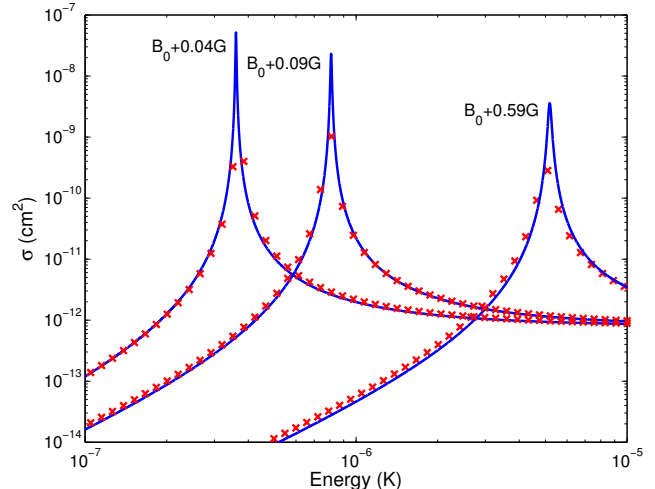


FIG. 2: (Color online) p -wave elastic scattering cross section for ^{40}K colliding in the $|9/2, -7/2\rangle$ channel as a function of collision energy at three different magnetic field strengths. The solid blue line corresponds to the pseudo potential model. The red crosses are from a coupled-channel calculation.

III. MEAN-FIELD THERMODYNAMICS

The stationary properties of a weakly attractive ultracold Fermi gas can be described by the BCS theory of superconductivity [7]. While trapped gases usually have anisotropic and inhomogeneous density distributions, for simplicity we consider here a spatially homogenous system.

In the following we review some standard results of BCS theory [42] to present the notation we use in the following paragraphs. The many body Hamiltonian for a system of fermions in the pairing approximation is given by

$$H = \sum_{ij} \langle i|K|j\rangle a_i^\dagger a_j + \frac{1}{2} \sum_{klmn} \langle kl|V|mn\rangle \left(\langle a_k^\dagger a_l^\dagger \rangle a_n a_m + a_k^\dagger a_l^\dagger \langle a_n a_m \rangle \right). \quad (8)$$

Here the a_i and a_i^\dagger are the usual fermion annihilation and creation operators, which obey the usual fermion anti-commutation rules, K is the single particle kinetic energy operator, and V is the interaction potential. The brackets $\langle \dots \rangle$ represent an average over the thermodynamic state of the system in the grand canonical ensemble where particle number is not fixed, $|i\rangle$ are single particle states and $|ij\rangle$ are two particle states. The finite temperature Green's functions of the system can be defined as

$$g_{rs}(\tau, \tau') = -\langle T_\tau [a_r(\tau) a_s^\dagger(\tau')] \rangle, \quad (9)$$

$$F_{rs}^\dagger(\tau, \tau') = -\langle T_\tau [a_r^\dagger(\tau) a_s^\dagger(\tau')] \rangle, \quad (10)$$

the latter representing pairing in the gas. Here T_τ is the imaginary time ordering operator that puts the smallest value of τ to right [42]. It is also often convenient to define a gap function

$$\Delta_{rs} = \sum_{ij} \langle a_i a_j \rangle \langle rs | V | ij \rangle, \quad (11)$$

which acts as the order parameter of our system.

By working in the momentum representation and considering a translationally invariant system we can write down the Heisenberg equations of motion for the Green's functions. The resulting equations can be Fourier transformed and combined with Eq. (11) to give

$$\Delta^*(\mathbf{p}) = - \int d^3q \langle \mathbf{p} | V | \mathbf{q} \rangle \frac{\Delta^*(\mathbf{q})}{2\epsilon_{\mathbf{q}}} \tanh(\beta \frac{\epsilon_{\mathbf{q}}}{2}), \quad (12)$$

and

$$\frac{N}{\mathcal{V}} = \frac{1}{2} \int d^3q \left[1 - \frac{E_q}{2\epsilon_{\mathbf{q}}} \tanh(\beta \frac{\epsilon_{\mathbf{q}}}{2}) \right], \quad (13)$$

where $\epsilon_{\mathbf{q}} = (E_q^2 + |\Delta(\mathbf{q})|^2)^{1/2}$, $E_q = \frac{q^2}{2m} - \mu$, \mathcal{V} is the

volume of the system, $\beta = \frac{1}{k_B T}$ and k_B is Boltzmann's constant. Equations (12) and (13) are often referred to as the gap equation and the density equation, respectively. These are the BCS equations for the system and must be solved simultaneously. Experiments are usually performed at constant temperature, which fixes β in our system. This leaves the chemical potential, μ , and $\Delta(p)$, as parameters to be solved for.

Using the potential of Eq. (1) the order parameter can be written as

$$\Delta^*(\mathbf{p}) = \sum_{m_1} \Delta_{m_1}^* \chi_{m_1}(p) Y_{1,m_1}^*(\hat{\mathbf{p}}), \quad (14)$$

where Δ_{m_1} and $\chi_{m_1}(p) = \langle p1, m_\ell | \chi_{1,m_\ell} \rangle$ represent components in the p -wave. We now drop the label ℓ in the subindex in the functions we have defined, since we will only be concerned with the p -wave, $\ell = 1$. By inserting this into Eq. (12) we arrive at a set of coupled equations for all components of the gap in the angular momentum basis

$$\Delta_{m_1}^* = - \int d^3q \sum_{m'_1} \frac{\chi_{m_1}(q) Y_{1,m_1}(\hat{\mathbf{q}}) \xi_{m_1} \Delta_{m'_1}^* \chi_{m'_1}(q) Y_{1,m'_1}^*(\hat{\mathbf{q}})}{2\epsilon_{\mathbf{q}}} \tanh \left[\frac{\beta}{2} \epsilon_{\mathbf{q}} \right]. \quad (15)$$

Experiments have shown the $m_1 = 1$ and $m_1 = -1$ states to be degenerate [24]. The degeneracy of the two components is due to the rotational symmetry of the system about the magnetic field axis. The parameter Δ_{m_1} for the $m_1 = 1$ and $m_1 = -1$ components can be written as

$$\Delta_{\pm 1} = \mp \frac{1}{\sqrt{2}} (\Delta_x \pm i \Delta_y), \quad (16)$$

where the magnitudes of these components are identical.

It is possible to reduce the set of three coupled nonlinear equations to two [43], so that we can write

$$\begin{pmatrix} \Delta_x^* \\ \sqrt{\frac{\xi_x}{\xi_z}} \Delta_z^* \end{pmatrix} = \begin{pmatrix} \langle \psi_x(\mathbf{q}), \psi_x(\mathbf{q}) \rangle & \langle \psi_x(\mathbf{q}), \psi_z(\mathbf{q}) \rangle \\ \langle \psi_z(\mathbf{q}), \psi_x(\mathbf{q}) \rangle & \langle \psi_z(\mathbf{q}), \psi_z(\mathbf{q}) \rangle \end{pmatrix} \times \begin{pmatrix} \Delta_x^* \\ \sqrt{\frac{\xi_x}{\xi_z}} \Delta_z^* \end{pmatrix}. \quad (17)$$

Here brackets $\langle \cdot, \cdot \rangle$ represent scalar products of two functions and should not be confused with a thermodynamic average. The functions are given by,

$$\psi_x(\mathbf{q}) = i \sqrt{\frac{3f(\mathbf{q})\xi_x}{4\pi}} \chi_{11}(q) \sin \theta \cos \phi, \quad (18)$$

and

$$\psi_z(\mathbf{q}) = i \sqrt{\frac{3f(\mathbf{q})\xi_z}{4\pi}} \chi_0(q) \cos \theta, \quad (19)$$

where for brevity we have defined

$$f(\mathbf{q}) = \frac{\tanh \left[\frac{\beta}{2} \epsilon_{\mathbf{q}} \right]}{\epsilon_{\mathbf{q}}}. \quad (20)$$

We have solved Eq. (17) for the resonance around 198.85 G in ^{40}K . We found that the off-diagonal matrix elements are several orders of magnitude smaller than the diagonal elements for densities of 10^{13} cm^{-3} to 10^{15} cm^{-3} . In this case neglecting the off-diagonal elements does not noticeably change the solution. A plot of the solutions to the BCS equations for ^{40}K is shown in Fig. 3, for the gap parameters, Δ_{m_1} and Fig. 4 for the chemical potentials μ . Previous work has used the Bose-Fermi [44, 45] model to study the thermodynamic properties of resonant p -wave gases [16, 18–20, 46]. We have calculated the chemical potential and gap parameters using both models and shown the results of the two models to be very similar throughout the crossover region [43].

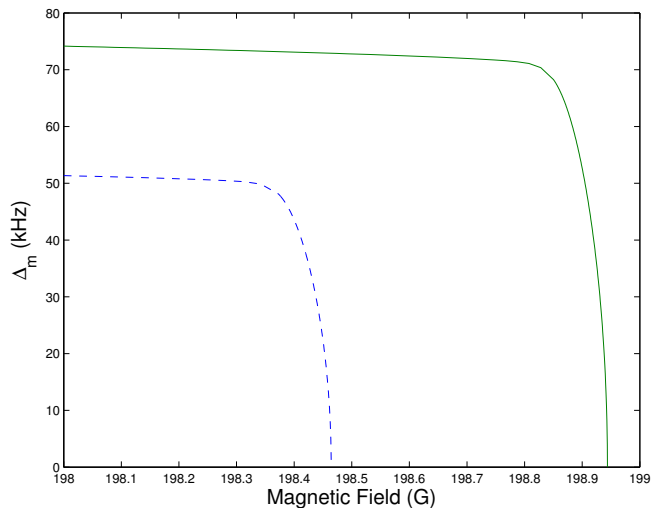


FIG. 3: (Color online) Variation of the parameter Δ_m with magnetic field for the p -wave resonance in ^{40}K for a density of 10^{13}cm^{-3} and a temperature of 70nK. The solid green line is the value of the $m = 0$ resonance and the dashed blue line is for the $|m| = 1$ resonance. There is no significant difference between the results obtained when coupling between the components is included and when the coupling is excluded.

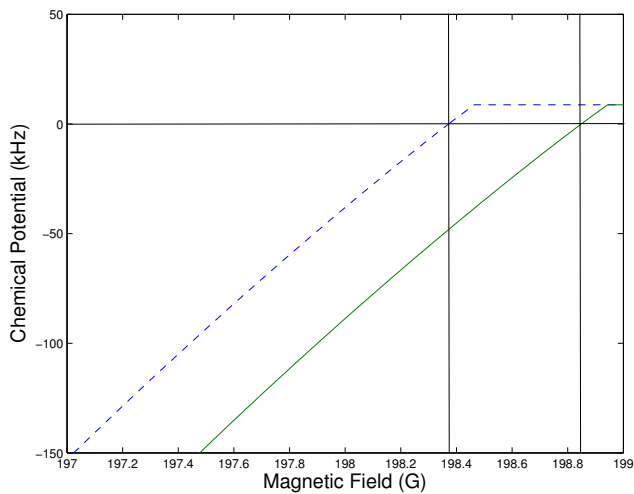


FIG. 4: (Color online) Values of the p -wave chemical potential for the resonance in ^{40}K for a density of 10^{13}cm^{-3} and a temperature of 70nK. The dashed blue line is the $|m_1| = 1$ resonance and the solid green line is the $m_1 = 0$ resonance. The values for coupled resonances and separated resonances are indistinguishable. The positions of the resonances are marked by the vertical lines.

IV. MEAN-FIELD DYNAMICS

A. Dynamics of molecule production

Experiments on the formation of molecules often use finite speed magnetic field variations to create molecules

from gases of ultra-cold fermions [8, 47–49]. This has stimulated theoretical research into studying the dynamics of molecule production in these gases [30, 50–57]. At the mean-field level the gas can be described by two correlation functions: the pair function, $\Phi_{ij}(t) = \langle a_j a_i \rangle_t$, and the one body density matrix $\Gamma_{ij}(t) = \langle a_j^\dagger a_i \rangle_t$. The brackets $\langle \dots \rangle_t$ represent a thermal average at time t . Their Heisenberg equations of motion in the momentum representation for a homogeneous system are [30]

$$i\hbar \frac{\partial}{\partial t} \Gamma(\mathbf{p}, t) = 2(2\pi\hbar)^{3/2} i \text{Im} (\Phi^*(\mathbf{p}, t) \langle \mathbf{p} | V | \Phi(t) \rangle) \quad (21)$$

$$i\hbar \frac{\partial}{\partial t} \Phi(\mathbf{p}, t) = \langle \mathbf{p} | H_{2B} | \Phi(t) \rangle - \langle \mathbf{p} | V | \Phi(t) \rangle \Gamma(-\mathbf{p}, t) (2\pi\hbar)^{3/2} - \langle \mathbf{p} | V | \Phi(t) \rangle \Gamma(\mathbf{p}, t) (2\pi\hbar)^{3/2}. \quad (22)$$

where due to translational invariance we have $\Gamma_{\mathbf{p}, \mathbf{p}} = \Gamma(\mathbf{p})\delta(0)$ and $\Phi_{\mathbf{p}, -\mathbf{p}} = \Phi(\mathbf{p})\delta(0)$. The initial correlation functions are related to the solutions of the BCS equations of Sect. III through

$$\frac{N}{\mathcal{V}} = \int \frac{d^3p}{(2\pi\hbar)^{3/2}} \Gamma(\mathbf{p}) \quad (23)$$

and

$$\Delta(q) = \int d^3q \langle \mathbf{p} | V | \mathbf{q} \rangle \Phi(\mathbf{q}) \quad (24)$$

These equations form a closed set of equations for the density distributions, without need for auxiliary parameters or constraints [30]. Dynamical equations can be written for the partial components of both the pair function and the one-body density matrix. For example, the component of the pair function is given by

$$\Phi_{\ell, m_\ell}(q, t) = i^\ell \int d\Omega Y_{\ell, m_\ell}^*(\Omega) \Phi(\mathbf{q}, t), \quad (25)$$

where Ω is the solid angle in \mathbf{q} . A similar expression can be written for the density matrix components, $\Gamma_{\ell, m_\ell}(q, t)$. This allows the angular integrals in the dynamic equations to be performed analytically, reducing the dimensionality of the numerical problem provided the contribution from higher partial waves is not significant. When the initial conditions allow the resonances to be treated separately the initial state of the gas is in either an $|m_1| = 1$ state or an $m_1 = 0$ state. At this level of approximation it is not possible to transfer population between these two components through the dynamics and we therefore treat them as individual cases. We study the case of a linear magnetic field sweep

$$B(t) = B_i - \dot{B}t \quad (26)$$

where B_i is the initial magnetic field above the resonance, $t = 0$ is the time at which the initial state is prepared and \dot{B} is the sweep rate. At some point the sweep will

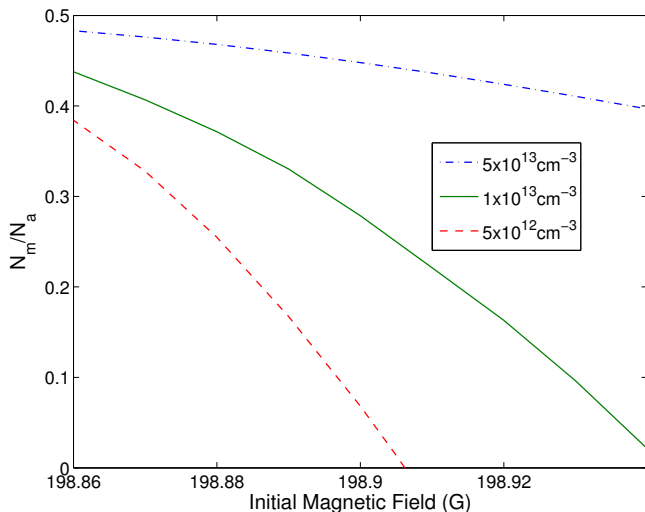


FIG. 5: (Color online) Variation of the molecular production efficiency in ^{40}K as the initial value of the magnetic field is varied. The different lines represent different densities. Higher densities give a larger production efficiency. The temperature is 70nK and the sweep rate is held constant at $\dot{B} = 60$ G/ms.

cease to produce molecules, so that we may choose a final magnetic field in the BEC side of the resonance where the molecule production has saturated.

The density of molecules at the end of the sweep can be calculated from a Wick expansion of the two-body correlation function. This can be approximately written as an overlap with the two-body bound state [30]

$$n_{\text{mol}} = \frac{1}{2} \left| \int d^3p \phi_{\text{b}}^*(\mathbf{p}) \Phi(\mathbf{p}) \right|^2, \quad (27)$$

where $\phi_{\text{b}}^*(\mathbf{p})$ is the two-body bound state wavefunction in the momentum representation obtained by solving the Schrödinger equation using the separable potential. In Eq. (27) the pair function, $\Phi(\mathbf{p})$ is evaluated at the final magnetic field strength of the sweep.

As a first approximation we retain the lowest order partial waves. The effect of adding in the higher partial waves can then be investigated. To study the dynamics of $m_1 = 0$ molecule formation in this approximation we retain the functions $\Phi_{10}(p, t)$ and $\Gamma_{00}(p, t)$.

We have investigated the variation in $m_1 = 0$ molecule production as a function of the initial magnetic field, B_i . In this case the temperature, atomic density and ramp speed of the magnetic field are held constant. The result is plotted in Fig. 5. As the initial magnetic field moves closer to the resonance position the molecule production increases. This is due to an increase in the pairing in the initial state of the gas, as can be seen from Fig. 3. Similarly, increasing the atomic density increases the production efficiency as shown in Fig. 6. We remark that our mean-field calculations predict a saturation of the molecule production efficiency at increasing density. This is an expected many-body effect, in con-

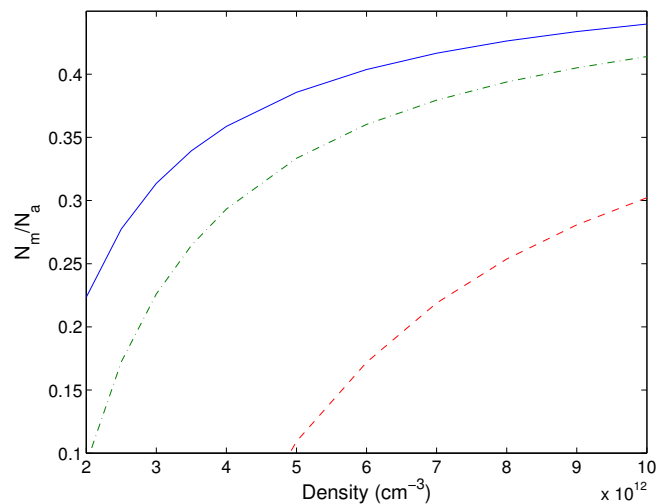


FIG. 6: (Color online) Variation of the molecular production in ^{40}K efficiency as the atomic density is varied. The sweep rate is held constant at $\dot{B} = 60$ G/ms. The lines represent temperatures of 70nK (solid blue), 100nK (dot-dashed green) and 200nK (dashed red).

trast to purely two-body calculations that would predict N_m/N_a to be linearly proportional to the density.

Investigating the variation of the production efficiency as a function of initial magnetic field proved to be difficult at low densities ($\sim 10^{12} - 10^{13} \text{ cm}^{-3}$). This is because the gap parameter quickly drops to zero on the BCS side of the resonance at these low densities. At such densities it should then be possible to approximate the production efficiency at the mean-field level with an instant projection of the initial pair state onto the bound state. This is because when the initial field is close to the resonance the quantities of interest will not evolve significantly before the final magnetic field is reached.

It has been shown by Iskin et al. [58] that for a harmonically trapped p -wave superfluid the central density is much larger than for the corresponding s -wave superfluid. This indicates that it may be feasible to reach higher densities in p -wave Fermi gases. Following this observation, we performed calculations setting the initial atomic density to a value well above those normally used in experiments (greater than 10^{14} cm^{-3}). In Fig. 7 we present calculations performed for a initial atomic density of 10^{15} cm^{-3} . These results show that it is possible to produce a significant number of molecules even when pairing in the initial state of the gas is not very large. This can be achieved by adjusting the sweep rate to lower and lower values, thus allowing for two-body correlations to build up during the sweep via intrinsically many-body processes. The closer the value of B_i is to the resonance the more difficult it is to influence the number of molecules produced by varying the sweep rate. This is because there is already a great amount of pairing in the gas and the production efficiency N_m/N_a can not exceed 0.5. On the other hand, at low ramp speeds the

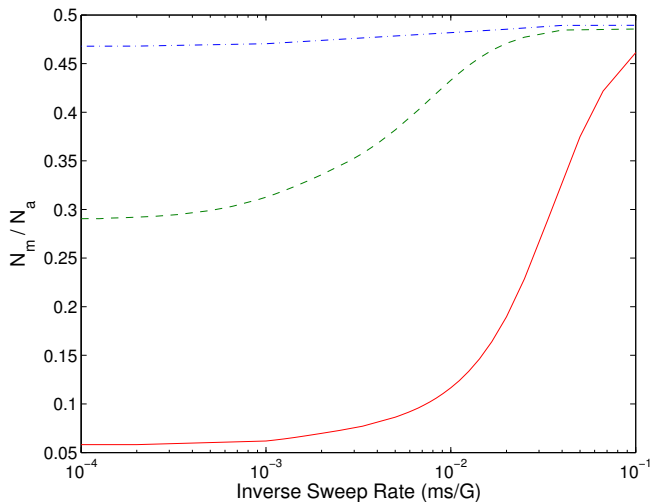


FIG. 7: (Color online) Variation of the molecular production efficiency in ^{40}K as the ramp speed is varied for a temperature of 70nK. The blue, dot-dashed curve refers to an atomic density of 10^{15} cm^{-3} and an initial magnetic field of 199 G. The green, dashed curve refers to an atomic density of 10^{15} cm^{-3} and an initial magnetic field of 200 G. The red, solid curve refers to an atomic density of $4 \times 10^{14} \text{ cm}^{-3}$ and an initial magnetic field of 200 G.

production efficiencies all converge and become independent of B_i , following the adiabatic value obtained from the thermodynamic state.

It may still be possible to produce molecules from a linear sweep of the magnetic field at lower densities. As a comparison, the molecule production at atomic densities of $4 \times 10^{14} \text{ cm}^{-3}$ as a function of inverse sweep rate has been plotted in Fig. 7 (solid, red line). The initial magnetic field has been set to 200G so that a direct comparison can be made with the dashed-green line. More molecules are produced relative to the production from an infinitely fast sweep for the lower density of $4 \times 10^{14} \text{ cm}^{-3}$. However, to achieve a similar net production efficiency as the 10^{15} cm^{-3} gas, the ramp speed will have to be set to significantly lower values where effects due to higher order correlation functions (not captured in the present mean-field approach) may become relevant.

To analyze how many molecules are actually produced during the dynamics, we show in Fig. 8 the fraction of molecules produced from a 500G/ms sweep subtracted from the fraction produced from a 10G/ms sweep. It can be seen that there is a maximum in the production efficiency at a certain value of the density. This peak increases in magnitude and moves to higher densities as the initial value of the magnetic field B_i is moved to higher fields. This shows that combinations of initial density and initial magnetic field can be picked to optimise the production efficiency.

We have checked that including higher partial wave components to study the dynamics does not significantly affect the production efficiencies reported here [43]. It ap-

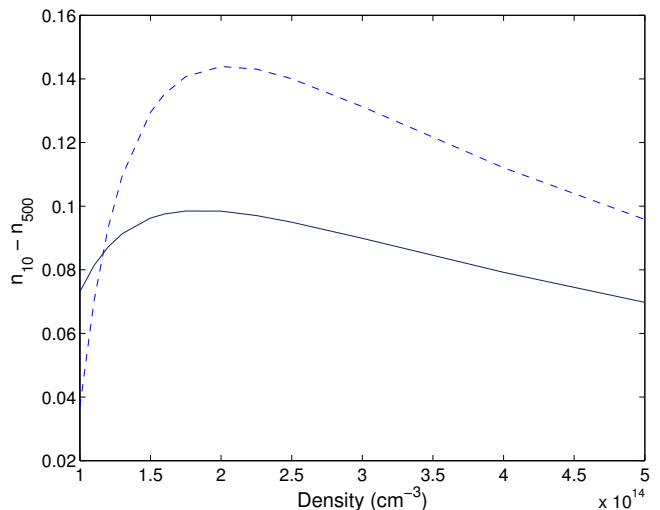


FIG. 8: The difference in the molecule production efficiency from a sweep of 10G/ms and a sweep of 500G/ms as a function of density. Here, $n_{\dot{B}}$ is the number of molecules over the number of atoms after a sweep at a speed equal to \dot{B} in G/ms for a temperature of 70nK. This shows how many molecules are actually produced during the dynamics. The dashed curve refers to an initial magnetic field position of $B_i = 199.3\text{G}$, while the lower curve refers to $B_i = 199.2\text{G}$. It can be seen there is an optimum density at which to produce molecules from the dynamics.

pears that retaining only the lowest ℓ components is sufficient to calculate the production at the mean-field level. Similar results are obtained for the $m_1 = 1$ molecules by allowing the initial state of the gas to be paired with $m_1 = 1$ symmetry.

B. Atom-molecule coherence

In experiments on s -wave molecule production, rapid sweeps of the magnetic field were used to probe the state of the Fermi gas in the region about the resonance. It was hypothesised that if the magnetic field was swept into the BEC side fast enough, such that the typical sweep time was less than the typical collision time, then it would be possible to extract information about the gas in the strongly interacting region [59]. The question then arises of how the state evolves after such a sweep. If the final state, held at a fixed field value, undergoes processes that significantly change it, then this method may not be a reliable way of probing the gas. For the s -wave it has been shown that under such a magnetic field variation the final molecule production efficiency will oscillate but with a small, decreasing amplitude [30]. We use an essentially identical method to show that this is also true in the p -wave and it would not be possible to observe atom-molecule coherence with this approach.

Fig. 9 shows the variation in the production efficiency as a function of time after such a magnetic field variation.

In this figure, the different lines correspond to different final magnetic fields. The variation in the molecule production over this time period is given as a percentage and seen to be on the order of 10^{-3} %, which is very small. The oscillations in the production are heavily damped with the oscillation frequency and damping rate increasing as the final magnetic field moves away from the resonance. For the case where the final field is located at 196.5 G the oscillations are not visible on the scale of the figure after 20 μ s.

In Fig. 10 the initial magnetic field is varied and the final magnetic field held constant. Again the oscillations for all detunings are on the order of 10^{-3} %. Both the frequency and amplitude of the oscillations increase as the initial field moves further from the resonance, but not significantly. It should be noted that this appears to be in contrast to the s -wave where the amplitude increases as the initial field moves towards the resonance [30]. However, in the s -wave studies the final field was generally chosen to be much further from the resonance position, and so corresponds to a BCS like state projected quickly onto a deeply bound BEC state. The near orthogonality between the initial and final states in such a case means that oscillations are likely to be small in the mean-field limit. In our results with the final field closer to the resonance position we see merely the change in the pairing between initial and final state reflected. In both cases the amplitude of the oscillations is very small (the results compared to in the s -wave correspond to a density of 1.5×10^{13} cm^{-3}).

We have also studied how the order parameter varies after such a magnetic field variation. In this case the gap parameter is a function of time defined by

$$\Delta(t) = \xi \int d^3q \langle \chi | \mathbf{q} \rangle \langle \mathbf{q} | \Phi(t) \rangle, \quad (28)$$

where we have used the separable potential to divide out a form factor from each side of the equation. We note that the value of the binding energy does not enter this equation directly. We compare this value against the value of the gap parameter when the system is in equilibrium at the final magnetic field position. We note that, in general, the quantity in Eq. (28) is complex. As for the case of the density variation, we have studied the effect of varying both the initial and final magnetic fields.

We plot the time evolution of the gap parameter in Fig. 11. The top and bottom panels refer to final magnetic fields of 197G and 198G, respectively. In each panel the different lines correspond to different initial magnetic field positions of 198.2G (top, red), 200.2G (middle, green) and 201.2G (bottom, blue). It can be seen that the closer the initial and final fields are to each other the closer the value of the gap parameter is to the stationary state value at the final magnetic field position, denoted here by Δ_{eq} . In all cases, the oscillations have a small amplitude and quickly decay. The real and imaginary parts of the gap parameter oscillate at a frequency that corresponds to the energy of the bound state at the final

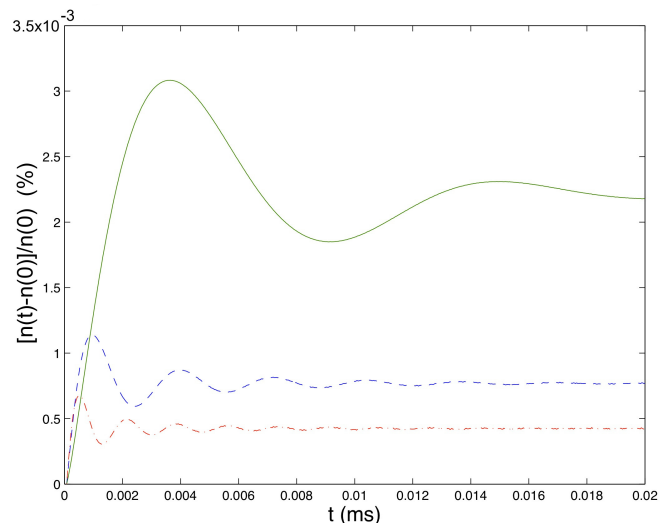


FIG. 9: (Color online) Evolution of the molecule production efficiency after an infinitely fast sweep of the magnetic field across the 198.85 G resonance in ^{40}K . The initial magnetic field is 199 G, just above the resonance. The different lines correspond to differing final magnetic fields of 198.5 G (solid, green line), 197.5 G (dashed, blue line) and 196.5 G (dot-dashed, red line). $n(t)$ is the density of molecules as a function of time where $n(0)$ is the density of molecules directly after the magnetic field variation.

magnetic field position. This is expected and serves as a test on the numerics. The value of oscillation frequency of the absolute value of the gap parameter increases as the initial magnetic field moves away from the resonance position and approximately corresponds to the sum of the final bound state energy and twice the initial chemical potential energy, a measure of the change in energy of the paired state during the sweep.

We conclude that it would not be feasible to observe atom-molecule oscillations in this p -wave resonance due to the small, rapidly decaying amplitude of the density oscillations. This is essentially the same conclusion reached in Szymańska et al. [30] but extends this result to the closed-channel dominated p -wave resonance in ^{40}K . This also suggests that the method of fast sweeps to probe a fermionic p -wave paired condensate would be a suitable method to probe the condensate were such conditions favourable.

V. DISCUSSION

We have studied the dynamics of p -wave Feshbach molecule formation by linear sweeps of the magnetic field within a mean-field approach. It turns out that the molecule production efficiency is highly dependent on the initial state of the gas. As the density increases it is increasingly possible to explore a range of initial magnetic field values, B_i . As the value of B_i moves away from the resonance and deeper into the BCS region it becomes

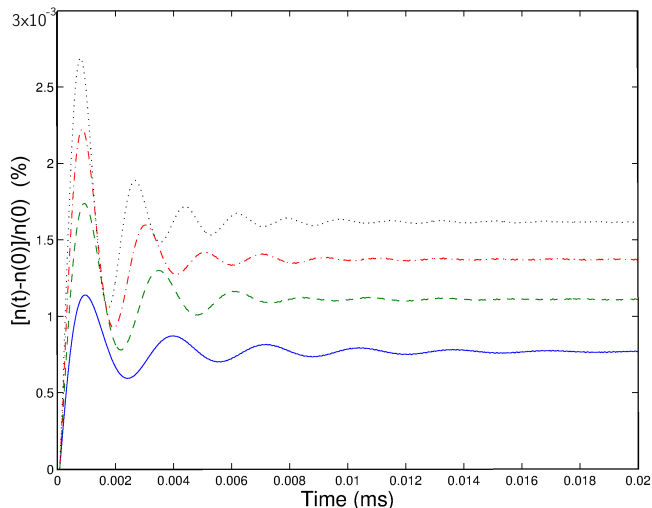


FIG. 10: (Color online) Evolution of the molecule production efficiency after an infinitely fast sweep of the magnetic field across the 198.85 G resonance in ^{40}K . The final field is held constant at 197.5 G. The different lines represent different initial magnetic fields of 199 G (solid, blue line), 199.5 G (dashed, green line), 200 G (dot-dashed, red line) and 200.5 G (dotted, black line). Other symbols are as defined in Fig. 9

easier to produce molecules through a sweep of the magnetic field if the density is high enough. Moreover, for a given magnetic field value there exists a density at which molecule production from a linear sweep is optimal. This is due to the fact that as the density increases so does the value of the molecule production from an instantaneous projection of the initial state onto the final molecular wave function. We have treated the $m_1 = 0$ and $|m_1| = 1$ molecules separately since even at relatively high density the thermodynamic states are well described separately. In turn this allows the dynamics to be treated as if the resonances were uncoupled. The initial assumption that the partial wave series for the dynamical functions will converge seems to be justified since adding higher partial waves has little effect on the production efficiency. We have also shown that, similarly to the case of an s -wave paired system [30], it would be very difficult to observe atom-molecule coherence as the result of a fast sweep experiment.

We note that our production efficiencies are generally reasonably high, and in our treatment a sizeable fraction of the atoms can be associated into molecules using experimentally realistic magnetic ramp speeds. However, we have not included relaxation processes into our treatment as such terms are beyond the mean-field theory we have used. Experiments to date on p -wave molecules have found them to be short lived, with lifetimes of between 2 and 20 ms [22, 25, 26, 28], due to dipolar relaxation processes [25] and three-body losses [46, 60, 61]. Our results indicate that small experimental molecular efficiencies cannot be explained by mean-field theory.

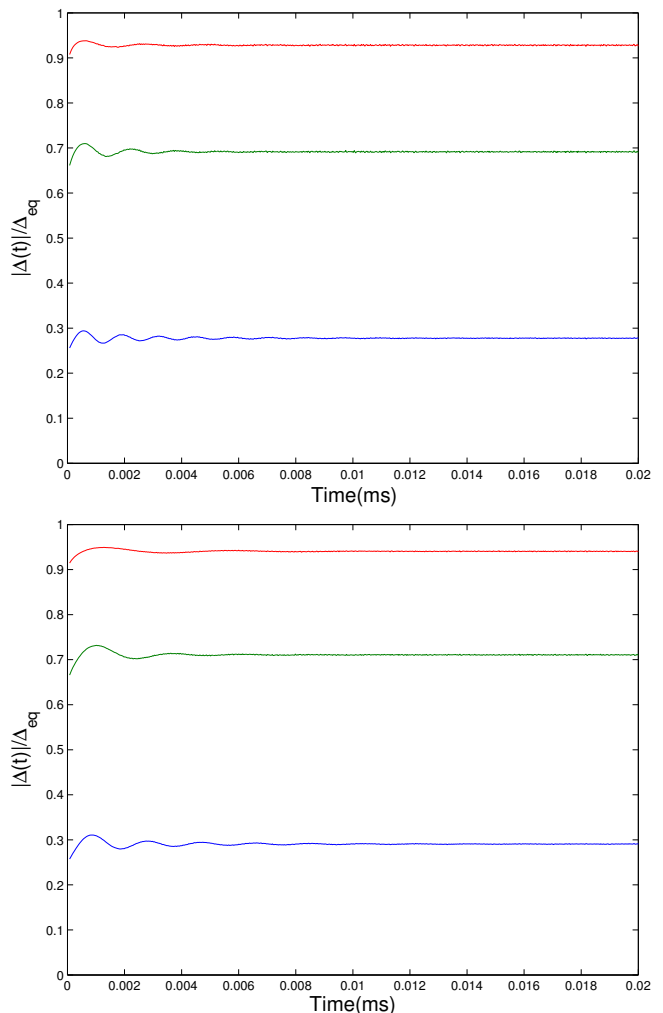


FIG. 11: (Color online) Variation of the quantity $|\Delta(t)|/\Delta_{eq}$ with time for final magnetic fields of 197 G (top panel) and 198 G (bottom panel). The different lines correspond to different initial magnetic field positions of 198.2 G (top, red), 200.2 G (middle, green) and 201.2 G (bottom, blue).

For single-component Fermi systems with p -wave interactions, several theoretical approaches predict the occurrence of quantum phase transitions (QPTs) in 2D [18, 19, 62] and 3D [63] between states with different molecular angular momenta, when the strength the interaction changes. The existence of such QPTs might be observable in cold Fermi gases by tuning their interaction through a Feshbach resonance, showing particular signatures in the momentum distribution [62, 64] or the size of the pairs [63, 65]; molecule formation might also be affected by the presence of the QPT. In the case of the resonance studied in this paper, however, the splitting between the $m = 0$ and $m = \pm 1$ resonances is large and appears to indicate that no QPT will occur under current experimental conditions [20], and furthermore that the resonances are approximately independent. To study molecule formation for other systems in which a QPT

may occur, our technique used in this paper might need to be extended to include beyond mean-field terms due to the difficulty in simulating a dynamical crossing of a QPT. Such an extension could be a generalisation of the approach used by Altman and Vishwanath [53] in the s -wave case, for example.

The authors acknowledge a significant contribution from T. Köhler to this work and are grateful to M. Szymańska for useful discussions. This work is funded by EPSRC grant EP/E025935/2, Spanish MICINN Project FIS2009-10061, CAM research consortium QUITEMAD, COST Action IOTA (MP1001), and a FP7 Marie Curie fellowship (J.M.-P.).

Appendix A: Modelling of the two-body interaction

Previous work has successfully used separable potentials with form factors of a Gaussian form to model the s -wave two-body interaction in the context of Feshbach resonances [30, 31]. This is convenient both analytically and numerically because Gaussian integrals can often be performed analytically. We wish to describe the system close to threshold and therefore choose the form factor to reflect the physics in this region. In the p -wave we choose the form factor to be

$$\langle \mathbf{p} | \chi_{m_1} \rangle = \frac{p\sigma_{m_1}}{\pi\hbar^{5/2}} e^{-\frac{p^2\sigma_{m_1}^2}{2\hbar^2}} Y_{1,m_1}(\hat{\mathbf{p}}) \quad (\text{A1})$$

which ensures the correct threshold behaviour of the bound and scattering states [66]. Here σ_m is a length scale associated with the range of the potential and $Y_{1,m_1}(\hat{\mathbf{p}})$ is the $\ell = 1$ spherical harmonic with a projection m_1 onto the chosen z -axis, in this case the magnetic field axis.

Using the form factor above and the low energy limit of the scattering amplitude it is possible to relate the scattering volume to the parameters of the separable potential amplitude, ξ_{m_1} defined in Eq. (1), and the form factor, Eq. (A1),

$$a_{1m_1} = 2\sigma_{m_1}^3 \frac{x}{1 + x/\sqrt{\pi}}, \quad (\text{A2})$$

where $x = m\xi_{m_1}/(4\pi\hbar^2\sigma_{m_1})$ is dimensionless, with m being the mass of the atom. Equation (6) for the bound state energy is then given by

$$1 + \frac{x}{\sqrt{\pi}} \left(1 - 2y^2 \left[1 - \sqrt{\pi}ye^{y^2} \operatorname{erfc}(y) \right] \right) = 0, \quad (\text{A3})$$

where $y = \sigma_{m_1}\sqrt{-mE_{-1}}/\hbar$, E_{-1} (< 0) is the bound state energy, and $\operatorname{erfc}(y) = \frac{2}{\sqrt{\pi}} \int_y^\infty \exp(-u^2) du$ is the complementary error function.

All of our calculations have been performed for the fermionic isotope ^{40}K . We have fixed the parameters of our separable potential using the experimental results of Refs. [24, 25]. To do this, we take the low energy expansion of the binding energy as given by Eq. (7) and parameterise the scattering volume as in Eq. (5). Close to the resonance we can expand the resonance formula as a series in powers of $(B - B_{\ell,m_\ell}^0)$, the terms of which can be directly read off from the expression given in Ref. [24] fixing the resonance parameters in Eq. (5). The values obtained are given in Table I.

$ m_\ell $	B_{ℓ,m_ℓ}^0 (G)	ΔB (G)	$a_{\ell m_\ell}^{\text{bg}}$ (a_B^3)
0	198.85	-21.9482	-1049850
1	198.373	-24.9922	-905505

TABLE I: Parameters used for modelling the two-body interaction (a_B indicates the Bohr radius.)

Equation (7) can be differentiated with respect to the magnetic field to give the magnetic moment of the molecules relative to the free atoms. This can be directly equated to the experimental values of the magnetic moment allowing the parameter σ_{m_1} to be calculated. Ref. [25] gives the magnetic moments of the molecules as

$$\left. \frac{\partial E}{\partial B} \right|_{m_1=0} = 188 \pm 2 \text{ kHz/G}, \quad (\text{A4})$$

and

$$\left. \frac{\partial E}{\partial B} \right|_{|m_1|=1} = 193 \pm 2 \text{ kHz/G}. \quad (\text{A5})$$

The corresponding range parameter is given by

$$\sigma_{m_\ell} = \frac{m\Delta B_{m_\ell}}{\sqrt{\pi}\hbar^2} a_{m_\ell}^{\text{bg}} \left. \frac{\partial E}{\partial B} \right|_{m_\ell}. \quad (\text{A6})$$

- [1] S. Giorgini, L. P. Pitaevskii, and S. Stringari, *Reviews of Modern Physics* **80**, 1215 (2008).
 [2] U. Fano, *Nuovo Cimento* **12**, 154 (1935).
 [3] H. Feshbach, *Ann. Phys.(N.Y.)* **5**, 357 (1958).
 [4] H. Feshbach, *Ann. Phys.(N.Y.)* **19**, 287 (1962).
 [5] E. Tiesinga, B. J. Verhaar, and H. T. C. Stoof, *Phys.*

- Rev. A* **47**, 4114 (1993).
 [6] C. Chin, R. Grimm, P. Julienne, and E. Tiesinga, *Rev. Mod. Phys.* **82**, 1225 (2010).
 [7] J. Bardeen, L. N. Cooper, and J. R. Schrieffer, *Phys. Rev.* **106**, 162 (1957).
 [8] C. A. Regal, C. Ticknor, J. L. Bohn, and D. S. Jin, *Nat.*

- ture **424**, 47 (2003).
- [9] R. Balian and N. R. Werthamer, *Phys. Rev.* **131**, 1553 (1963).
- [10] P. Wolfle, *Reports on Progress in Physics* **42**, 269 (1979).
- [11] S. Godfrey and R. Kokoski, *Phys. Rev. D* **43**, 1679 (1991).
- [12] M. Baranov, Y. Kagan, and M. Kagan, *Pis'ma Zh. Éksp. Teor. Fiz.* **64**, 273 (1996), [*Journal of Experimental and Theoretical Physics Letters* **64**, 301 (1996)], URL <http://dx.doi.org/10.1134/1.567187>.
- [13] D. V. Efremov and L. Viverit, *Phys. Rev. B* **65**, 134519 (2002).
- [14] J. Mur-Petit, A. Polls, M. Baldo, and H.-J. Schulze, *Phys. Rev. A* **69**, 023606 (2004).
- [15] J. Mur-Petit, A. Polls, M. Baldo, and H.-J. Schulze, *Journal of Physics B: Atomic, Molecular and Optical Physics* **37**, S165 (2004).
- [16] T.-L. Ho and R. B. Diener, *Phys. Rev. Lett.* **94**, 090402 (2005).
- [17] Y. Ohashi, *Phys. Rev. Lett.* **94**, 050403 (2005).
- [18] C.-H. Cheng and S.-K. Yip, *Phys. Rev. Lett.* **95**, 070404 (2005).
- [19] V. Gurarie, L. Radzihovsky, and A. V. Andreev, *Phys. Rev. Lett.* **94**, 230403 (2005).
- [20] V. Gurarie and L. Radzihovsky, *Ann. Phys.* **322**, 2 (2007).
- [21] C. A. Regal, C. Ticknor, J. L. Bohn, and D. S. Jin, *Phys. Rev. Lett.* **90**, 053201 (2003).
- [22] J. Zhang, E. G. M. van Kempen, T. Bourdel, L. Khaykovich, J. Cubizolles, F. Chevy, M. Teichmann, L. Tarruell, S. J. J. M. F. Kokkelmans, and C. Salomon, *Phys. Rev. A* **70**, 030702 (2004).
- [23] C. H. Schunck, M. W. Zwierlein, C. A. Stan, S. M. F. Raupach, W. Ketterle, A. Simoni, E. Tiesinga, C. J. Williams, and P. S. Julienne, *Phys. Rev. A* **71**, 045601 (2005).
- [24] C. Ticknor, C. A. Regal, D. S. Jin, and J. L. Bohn, *Phys. Rev. A* **69**, 042712 (2004).
- [25] J. P. Gaebler, J. T. Stewart, J. L. Bohn, and D. S. Jin, *Phys. Rev. Lett.* **98**, 200403 (2007).
- [26] J. Fuchs, C. Ticknor, P. Dyke, G. Veeravalli, E. Kuhnle, W. Rowlands, P. Hannaford, and C. J. Vale, *Phys. Rev. A* **77**, 053616 (2008).
- [27] S. T. Thompson, E. Hodby, and C. E. Wieman, *Phys. Rev. Lett.* **95**, 190404 (2005).
- [28] Y. Inada, M. Horikoshi, S. Nakajima, M. Kuwata-Gonokami, M. Ueda, and T. Mukaiyama, *Phys. Rev. Lett.* **101**, 100401 (2008).
- [29] R. A. W. Maier, C. Marzok, C. Zimmermann, and P. W. Courteille, *Phys. Rev. A* **81**, 064701 (2010).
- [30] M. H. Szymańska, B. D. Simons, and K. Burnett, *Phys. Rev. Lett.* **94**, 170402 (2005).
- [31] M. H. Szymańska, K. Góral, T. Köhler, and K. Burnett, *Phys. Rev. A* **72**, 013610 (2005).
- [32] J. R. Taylor, *Scattering Theory* (Dover, New York, 2006).
- [33] B. H. Bransden and C. J. Joachain, *Physics of Atoms and Molecules* (Prentice Hall, 2003).
- [34] R. G. Newton, *Scattering Theory of Wave and Particles* (Dover, New York, 2002).
- [35] A. J. Moerdijk, B. J. Verhaar, and A. Axelsson, *Phys. Rev. A* **51**, 4852 (1995).
- [36] K. B. Gubbels and H. T. C. Stoof, *Phys. Rev. Lett.* **99**, 190406 (2007).
- [37] B. Gao, *J. Phys. B: Atomic, Molecular and Optical Physics* **37**, 4273 (2004).
- [38] F. Chevy, E. G. M. van Kempen, T. Bourdel, J. Zhang, L. Khaykovich, M. Teichmann, L. Tarruell, S. J. J. M. F. Kokkelmans, and C. Salomon, *Phys. Rev. A* **71**, 062710 (2005).
- [39] D. E. Manolopoulos, *J. Chem. Phys.* **85**, 6425 (1986).
- [40] H. T. C. Stoof, J. M. V. A. Koelman, and B. J. Verhaar, *Phys. Rev. B* **38**, 4688 (1988).
- [41] S. Falke, H. Knöckel, J. Friebe, M. Riedmann, E. Tiemann, and C. Lisdat, *Phys. Rev. A* **78**, 012503 (2008).
- [42] A. L. Fetter and J. D. Walecka, *Quantum Theory of Many-Particle Systems* (Dover, 2003).
- [43] L. Austen, *PhD thesis* (University College London, 2011).
- [44] M. Holland, S. J. J. M. F. Kokkelmans, M. L. Chiofalo, and R. Walser, *Phys. Rev. Lett.* **87**, 120406 (2001).
- [45] E. Timmermans, K. Furuya, P. W. Milonni, and A. K. Kerman, *Phys. Lett. A* **285**, 228 (2001).
- [46] J. Levinsen, N. R. Cooper, and V. Gurarie, *Phys. Rev. Lett.* **99**, 210402 (2007).
- [47] K. E. Strecker, G. B. Partridge, and R. G. Hulet, *Phys. Rev. Lett.* **91**, 080406 (2003).
- [48] J. Cubizolles, T. Bourdel, S. J. J. M. F. Kokkelmans, G. V. Shlyapnikov, and C. Salomon, *Phys. Rev. Lett.* **91**, 240401 (2003).
- [49] S. Jochim, M. Bartenstein, A. Altmeyer, G. Hendl, C. Chin, J. H. Denschlag, and R. Grimm, *Phys. Rev. Lett.* **91**, 240402 (2003).
- [50] R. A. Barankov and L. S. Levitov, *Phys. Rev. Lett.* **93**, 130403 (2004).
- [51] R. A. Barankov, L. S. Levitov, and B. Z. Spivak, *Phys. Rev. Lett.* **93**, 160401 (2004).
- [52] A. V. Andreev, V. Gurarie, and L. Radzihovsky, *Phys. Rev. Lett.* **93**, 130402 (2004).
- [53] E. Altman and A. Vishwanath, *Phys. Rev. Lett.* **95**, 110404 (2005).
- [54] B. Dobrescu and V. Pokrovsky, *Phys. Lett. A* **350**, 154 (2006).
- [55] I. Tikhonenkov, E. Pazy, Y. B. Band, M. Fleischhauer, and A. Vardi, *Phys. Rev. A* **73**, 043605 (2006).
- [56] S. Matyjaśkiewicz, M. H. Szymańska, and K. Góral, *Phys. Rev. Lett.* **101**, 150410 (2008).
- [57] V. Gurarie, *Phys. Rev. A* **80**, 023626 (2009).
- [58] M. Iskin and C. J. Williams, *Phys. Rev. A* **77**, 041607 (2008).
- [59] C. A. Regal, M. Greiner, and D. S. Jin, *Phys. Rev. Lett.* **92**, 040403 (2004).
- [60] M. Jona-Lasinio, L. Pricoupenko, and Y. Castin, *Phys. Rev. A* **77**, 043611 (2008).
- [61] J. Levinsen, N. R. Cooper, and V. Gurarie, *Phys. Rev. A* **78**, 063616 (2008).
- [62] S. S. Botelho and C. A. R. Sá de Melo, *Journal of Low Temperature Physics* **140**, 409 (2005), ISSN 0022-2291.
- [63] M. Iskin and C. A. R. Sá de Melo, *Phys. Rev. Lett.* **96**, 040402 (2006).
- [64] S. M. A. Rombouts, J. Dukelsky, and G. Ortiz, *Phys. Rev. B* **82**, 224510 (2010).
- [65] S. Lerma H., S. M. A. Rombouts, J. Dukelsky, and G. Ortiz, *Phys. Rev. B* **84**, 100503 (2011).
- [66] C. Lovelace, *Phys. Rev.* **135**, B1225 (1964).